A simple model of adsorption by swelling porous materials: application of a density functional approach

2001 J. Phys.: Condens. Matter 13 6151

(http://iopscience.iop.org/0953-8984/13/28/301)

INSTITUTE OF PHYSICS PUBLISHING JOURNAL OF PHYSICS: CONDENSED MATTER

J. Phys.: Condens. Matter **13** (2001) 6151–6164 PII: S0953-8984(01)22983-X

A simple model of adsorption by swelling porous materials: application of a density functional approach

Andrzej Patrykiejew[1,4], **Stefan Sokołowski**[1,4], **Zofia Sokołowska**[2] **and Orest Pizio**[3]

[1] Department for the Modelling of Physico-Chemical Processes,
Maria Curie-Skołodowska University, 20031 Lublin, Poland
[2] Institute of Agrophysics, Polish Academy of Sciences, 20257 Lublin, Doświadczalna 4, Poland
[3] Institute de Química de la UNAM, Coyoàcan 04510, México DF, Mexico

E-mail: zosia@maja.ipan.lublin.pl (Z Sokołowska) and pizio@servidor.unam.mx (O Pizio)

Received 16 March 2001, in final form 5 June 2001
Published 29 June 2001
Online at stacks.iop.org/JPhysCM/13/6151

Abstract

We apply a density functional approach to describe adsorption of fluids by swelling porous materials. We investigate adsorption at supercritical temperatures, and discuss possible changes in the phase behaviour of the fluid which result from the volume changes of the pores during the adsorption process. In particular, we show that the swelling may cause splitting of the capillary condensation hysteresis loop into two branches; the first of them is connected with the capillary condensation in a 'collapsed' pore and the second one is a result of the swelling.

1. Introduction

A fundamental question asked in theoretical studies of confined fluids is how the phase transitions are affected by the state conditions of the adsorbed fluid and by pore variables, such as pore geometry and size and molecular structure of the walls; cf. the review papers [1–4]. The calculations that have to be performed to answer the above question are usually carried out by fixing the geometry of the pore and varying the state condition of the fluid. Obviously, in performing calculations one assumes that the pore size parameter(s) are independent of the amount of confined fluid. However, there are cases of adsorbents for which the above assumption may be not valid. Typical examples are gels and polymer gels that are commonly used in industrial, analytical and domestic applications, such as ion exchangers, coatings, nappies and fillings in chromatography. These substances swell when immersed in fluids [5, 6]. The swelling may also occur during adsorption of vapours by these adsorbents. Several theories have been proposed to describe equilibrium swelling of gels immersed in fluids [6–12].

[4] http://hermes.umcs.lublin.pl/~czmpf.

Another class of swelling adsorbents is composed of certain clay minerals. Clays, such as smectites and vermiculites, are widely spread in soils and are often used as adsorbents (e.g. in the oil industry) and supports for catalysts [13–15]. They are built of negatively charged sheets, which are held together by charge-balancing interlayer cations. In the presence of vapours of some polar substances (e.g. water and some organic substances), the interlayer cations have a strong tendency to hydrate (solvate), thereby forcing the layers to move apart. Consequently, adsorption isotherms exhibit jumps, because an additional amount of adsorbate may then occupy the space between the layers. Obviously, swelling can also occur during adsorption from solutions.

Several computer simulation studies of adsorption properties of clay minerals have been reported in the literature; see e.g. references [16–23]. In simulations, the possibility of changing interlayer spacing between sheets of a clay has been accounted for by treating the two pore walls as huge, interacting particles. The distance between them (and also their relative orientation; cf. [20]) could change during simulation runs; cf. for example reference [21]. In contrast to the sophisticated models used in simulations, interpretation of experimental adsorption data on water vapour [14] has usually been based on a phenomenological approach due to Van Olphen [24, 25], according to which the energy of the interactions between two sheets of a clay is the difference between the energy of hydration of the pore walls and the electrostatic energy between the pore walls.

The principal aim of this work is to propose a simple method to describe adsorption in slit-like pores, whose width, H, can vary during the adsorption process. Recently van Swol and co-workers [26–28] have proposed application of a kind of density functional theory to study the swelling of colloidal systems. To describe such systems, van Swol and co-workers computed the grand canonical potential for a set of distances between two (huge) colloidal particles, modelled as flat walls. For a stable phase, characterized by a given value of the distance between two colloidal particles H, the grand potential had to reach its absolute minimum value. In their treatment, van Swol and co-workers [26–28] also allowed for direct colloid–colloid interactions, modelling them via a potential of a Lennard-Jones (9, 3) type.

The approach considered here is different. We consider a function relating the pore width H to the amount of adsorbed fluid Γ, normalized per surface area of a single pore wall. This function is selected so as to mimic some experimental data on adsorption from gaseous [14, 29–33] and liquid [34, 35] phases, as well as simulational observations [19–22], but the particular form used in this work has, in fact, no theoretical justification. Moreover, although according to experiments the change of the pore width can occur in a series of discrete steps [14], we only consider the case of the function $H = H(\Gamma)$ exhibiting a single step. However, the introduction of such a function modifies the external potential field term in the density functional and in minimizing the grand potential we must explicitly take into account the assumed dependence of H on Γ.

The next section of our work contains a brief description of the theoretical procedures. The specific calculations are carried out for several model systems and for two regimes. In the first regime, we consider adsorption at temperatures higher than the bulk critical temperature. Following this, we present the results at low temperatures, at which the phenomenon of capillary condensation takes place. We show that the proposed model can lead to qualitative modifications of the phase behaviour of the confined fluid.

2. Theoretical procedure

Figure 1 shows changes in the average width of a slit-like pore during adsorption of CH_3CN on a sample of montmorillonite at 293 K [14, 32, 33]. The curve displayed here was evaluated

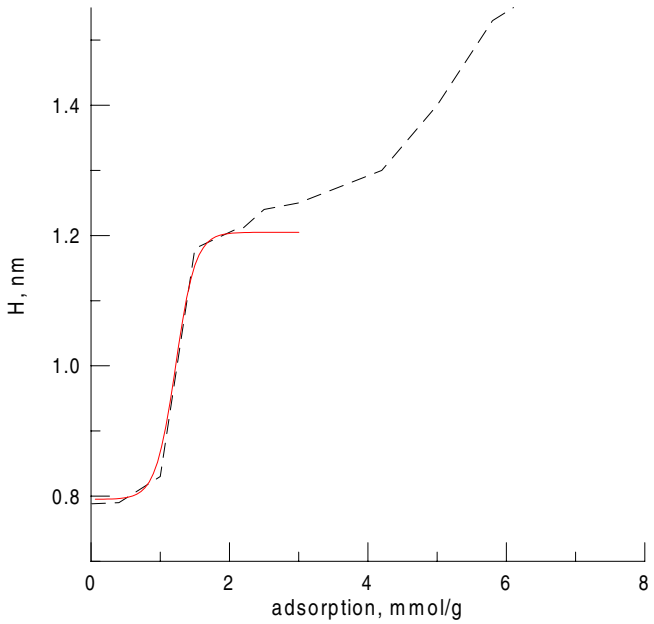

Figure 1. Changes of the pore width observed during adsorption of CH_3CN by montmorillonite, evaluated from experimental data [14, 32, 33] (dashed line) and the fit of the first step of the experimental curve with equation (1) (solid line). The parameters of equation (1) are given in the text.

from the adsorption isotherms of CH_3CN and from the dependence of the pore width on the relative pressure of CH_3CN, reported in [32, 33] (cf. also figures 124 and 125 in [14]). This curve exhibits two steps, but we only consider the first one. This step corresponds to an increase of the average pore width H from approximately 0.8 nm to about 1.2 nm. These changes can be described by the function

$$H = H_0 + H_1 \frac{1 - \exp[-\alpha(\Gamma - G)]}{1 + \exp[-\alpha(\Gamma - G)]} \tag{1}$$

where α, H_0, H_1 and G are parameters. In other words we model the variation of the pore width H with the amount of adsorbed gas Γ using an arcsine-type function; for adsorption $\Gamma = G$, the pore width equals $H = H_0$. In the case of the curve given in figure 1, the parameters of equation (1) fitting the experimental data are: $H_0 = 1.00$ nm, $H_1 = 0.205$ nm, $\alpha = 7$ g mmol^{-1} and $G = 1.22$ mmol g^{-1} (the experimental adsorption data are expressed in mmol g^{-1}).

In our approach we assume that the pore walls are energetically homogeneous—that is, the potential exerted by a single wall, v', is a function of the normal distance, z, only. The external field due to both pore walls

$$v(z; H) = v'(-H/2 - z) + v'(H/2 - z) \tag{2}$$

depends on the pore width and thus on Γ. We model $v'(x)$ using the Lennard-Jones function

$$v'(x) = \begin{cases} \varepsilon_s[(z_0/x)^9 - (z_0/x)^3] & x > 0 \\ \infty & \text{otherwise.} \end{cases} \tag{3}$$

The fluid particles interact via a truncated Lennard-Jones potential:

$$u(r) = \begin{cases} \varepsilon[(\sigma/r)^{12} - (\sigma/r)^6] & r < r_{cut} \\ 0 & \text{otherwise} \end{cases} \tag{4}$$

where r_{cut} is the cut-off distance and σ is the Lennard-Jones diameter. Hereafter we use σ and ε as the units of length and energy, respectively. We also define the reduced temperature as $T^* = kT/\varepsilon$. The grand potential functional $\Omega[\rho]$ is expressed as [36]

$$\Omega[\rho] = F[\rho] + \int \{v(z; H) - \mu\}\rho(z)\, \mathrm{d}\boldsymbol{r} \tag{5}$$

where $F[\rho]$ and μ are the configurational free energy and the configurational chemical potential of the fluid, respectively, and $\rho(z)$ is the local density. The equilibrium value of Ω is obtained by minimizing the functional, at a constant temperature, chemical potential and volume of a reservoir in which the swelling pore is immersed.

The free-energy functional $F[\rho]$ consists of two independent parts: an ideal-gas part, F^{id}, and an excess part. The ideal contribution has the form

$$F^{id}/kT = \int \rho(z)[\ln \rho(z) - 1]\, \mathrm{d}\boldsymbol{r}.$$

Although a non-perturbative density functional approach has been proposed recently [37], we apply here a classical method [36, 38], according to which the excess Helmholtz free energy is divided into a reference hard-sphere part and an attractive part: $F^{ex} = F^{ex,hs} + F^{ex,att}$. We have used the Tarazona approach [38] to evaluate the excess free-energy functional for hard spheres. Thus

$$F^{ex,hs}[\rho] = \int \rho(z) f^{hs}[\tilde{\rho}(z)]\, \mathrm{d}\boldsymbol{r} \tag{6}$$

where f^{hs} denotes the free energy per particle, resulting from the Carnahan–Starling equation of state, and $\tilde{\rho}(z)$ is the weighted density. The attractive energy contribution to the free-energy functional is determined by invoking a mean-field approximation; thus

$$F^{ex,att} = \frac{1}{2} \int \int \rho(z)\rho(z') u_a(|\boldsymbol{r} - \boldsymbol{r}'|)\, \mathrm{d}\boldsymbol{r}\, \mathrm{d}\boldsymbol{r}' \tag{7}$$

where the division of the Lennard-Jones potential, equation (4), into attractive and repulsive parts has been performed according to the Weeks, Chandler and Andersen recipe [39].

The amount of confined fluid is

$$\Gamma = \int \rho(z)\, \mathrm{d}z \tag{8}$$

where the integration range is not constant. Because the local density $\rho(z)$ also depends on the pore width, the calculation of Γ must be performed self-consistently while minimizing the functional Ω. The density profile equation, obtained from the condition $\delta\Omega/\delta\rho(z) = 0$, is

$$\mu_s = \mu + \mathcal{C} f_s = kT \ln \rho(z) + v(z; H) + f^{hs}[\tilde{\rho}(z)] + \int \rho(z') \frac{\delta f^{hs}[\tilde{\rho}(z')]}{\delta\rho(z)}\, \mathrm{d}z' + \int \rho(z') u_a(|\boldsymbol{r} - \boldsymbol{r}'|)\, \mathrm{d}\boldsymbol{r}'. \tag{9}$$

This is formally the same as the usual equation, but the value of the chemical potential is shifted by a solvation work term. In the above equation $\mathcal{C} = \partial H/\partial\Gamma$ and

$$f_s = \int \rho(z')[\mathrm{d}v'(H/2 - z')/\mathrm{d}z']\, \mathrm{d}z'$$

is the contribution due to the solvation force. The configurational chemical potential of a bulk fluid of density ρ_b is

$$\mu = kT \ln \rho_b + f^{hs}(\rho_b) + \rho_b[\partial f^{hs}(\rho_b)/\partial \rho_b] + \rho_b \int u_a(r)\, \mathrm{d}\boldsymbol{r}.$$

3. Results and discussion

Numerical solutions of equation (9) have been obtained by using an iterative procedure with a Picard mixing scheme [40] on a grid with the mesh size 0.02σ. After each iteration the value of Γ was evaluated and a new value of the pore width H was determined from equation (1). The next iteration was carried out using this new H-value and thus by using the redefined potential (2). The iterations were continued until the maximum deviation between two consecutive solutions $\rho(z)/\rho_b$ was smaller than 10^{-5}.

We first carried out model calculations of the adsorption of a fluid at a high temperature. The results presented in figure 1 are at the reduced temperature $T^* = 1.5$, which is higher than the bulk reduced critical temperature (the critical temperature, resulting from the bulk counterpart of the theory, is $T^*_{cb} \simeq 1.32$). In performing these calculations, we have fixed some parameters of the model; their values were: $z_0 = 0.5$, $\varepsilon_s/\varepsilon = 6$, $H_0 = 5$ and $H_1 = 1$. The two remaining parameters, namely α and G, were varied. The parameter G characterizes the value of the adsorption at which the pore width equals H_0; the parameter α changes the steepness of the variation of the pore width with the amount of adsorbed fluid.

Figure 2(a) illustrates changes in the density distribution with the bulk density, ρ_b, for $\alpha = 5$ and $G = 0.5$. The increase of the bulk density not only causes the development of a layered structure of the adsorbed fluid, but also leads to an increase of the pore width. At the bulk density 0.5, the adsorbed film that fills the pore causes an increase of its width to almost its maximum value of 6 (in units of σ). However, the filling of the pore and the increase of its width are continuous. Indeed, the adsorption isotherm labelled '1' in figure 2(b) and evaluated for the same system as the density profiles in figure 2(a) is smooth. Similarly, the increase of the pore width with the bulk density is depicted by a smooth line; cf. figure 2(c). Note that the pore width H attains a plateau at moderate bulk densities, $\rho_b \approx 0.25$.

When the parameter α is kept constant, $\alpha = 5$, but the value of G increases to 4 and the entire adsorption isotherm shifts down; cf. the line with the label '2' in figure 2(b). The explanation for such behaviour is quite obvious: if α is high enough, the dependence of H on G exhibits a very fast but continuous rise for the values of Γ close to G. At rather high bulk fluid density $\rho_b = 0.85$, the adsorption in the system under study is close to 3, i.e. it is much lower than the value of G. Significant change in the pore width can eventually be observed at much higher values of the bulk density. Inspecting the dependence of H on the bulk gas density (see figure 2(c)), we see that over the entire range of bulk densities investigated the pore width is almost exactly equal to its minimum value. The adsorption isotherm and the dependence of H on ρ_b shown in figures 2(b) and 2(c) as the curves labelled '3' are for $\alpha = 5$ and $G = 2$, i.e. the value of G is intermediate between those characterizing the systems discussed so far. The adsorption isotherm exhibits a very sharp but continuous rise at a bulk density close to 0.45; at the same bulk density the pore width changes significantly, but also continuously.

The value of α changes the steepness of the function (1); a higher value of α forces more abrupt changes of H for values of the adsorption close to G. If we now compare the adsorption isotherms obtained for $\alpha = 5$ and $G = 2$ (curve 3) and for $\alpha = 10$ and $G = 2$ (curve 4), we find an evidently sharper (but still continuous) adsorption rise for the system characterized by $\alpha = 10$. Similar behaviour is also seen in figure 2(c). It is thus not surprising that lowering the value of α (while keeping G constant) causes that the adsorption isotherm and the function

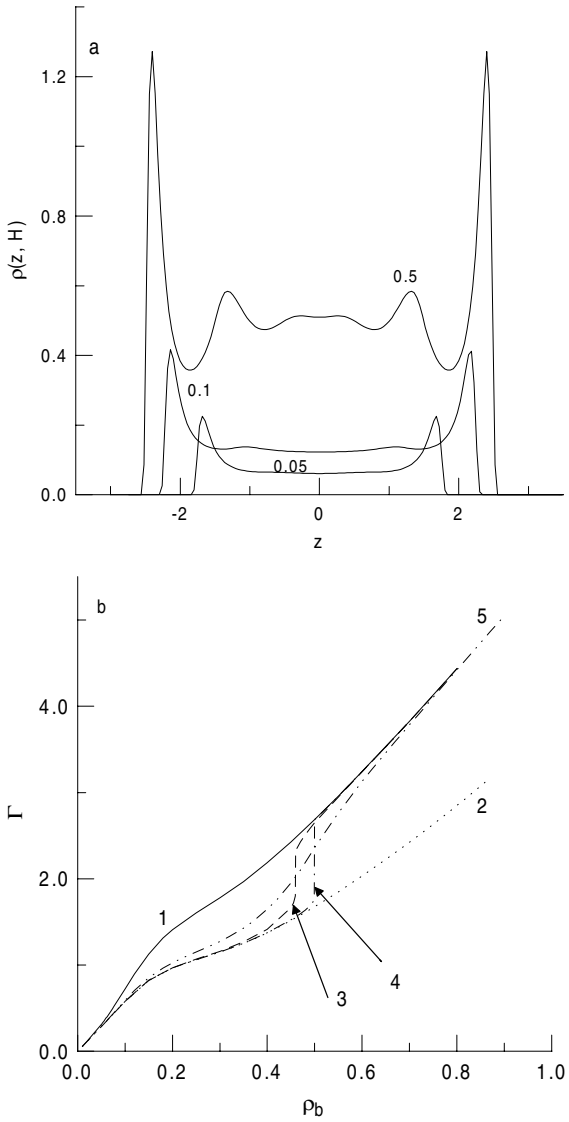

Figure 2. (a) Density profiles at bulk densities 0.05, 0.1 and 0.5 for the system with $H_0 = 5$, $H_1 = 1$, $G = 0.5$, $\alpha = 5$. ((b), (c)) Adsorption isotherms (b) and the dependence of the pore width H on the bulk density (c) for the following systems: $G = 0.5$ and $\alpha = 5$ (1); $G = 4$ and $\alpha = 5$ (2); $G = 2$ and $\alpha = 5$ (3); $G = 2$ and $\alpha = 10$ (4); and $G = 2$ and $\alpha = 2$ (5). The values of the remaining parameters of the model were as follows: $z_0 = 0.5$, $\varepsilon_s/\varepsilon = 6$, $H_0 = 5$, $H_1 = 1$, $T^* = 1.5$.

describing the dependence of the pore width on the bulk density (cf. the curves labelled '5' in figures 2(b) and 2(c)) to become smoother.

At low enough temperatures, the fluid undergoes a liquid–gas transition. The critical temperature for a fluid confined in a slit-like pore is lower than its bulk critical temperature and the entire phase coexistence line of the confined fluid is shifted towards lower temperatures. This phenomenon is known as capillary condensation. The lowering of the critical temperature and the hysteresis loop depend on the pore width. Therefore it is of interest to investigate how

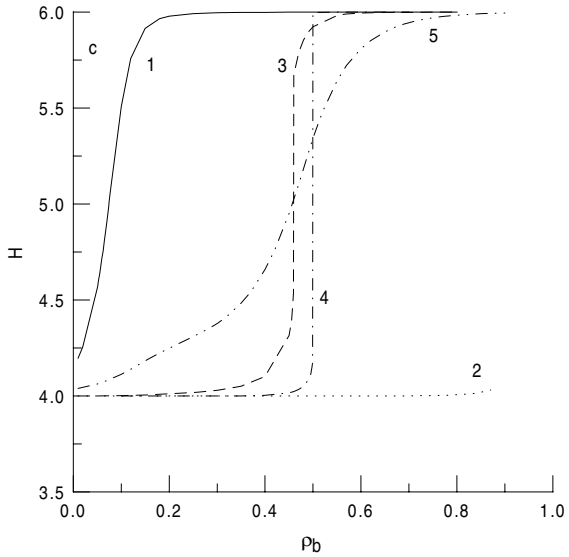

Figure 2. (Continued)

the adsorption and the critical properties of the fluid are modified when the pore width is allowed to vary with the amount adsorbed. Model calculations have been carried out assuming that $z_0 = 0.5$, $\varepsilon_s/\varepsilon = 6$, $H_0 = 5$. The parameter ε_s was set high enough to ensure a low wetting temperature of a fluid adsorbed at a single wall, but also to avoid problems connected with the occurrence of layering transitions in the system. Figure 3 displays examples of adsorption isotherms for a non-swelling system, i.e. for $H_1 = 0$. Here the width of the pore is equal to the average pore width of the systems investigated below. We have plotted two hysteresis branches; the equilibrium transition point (evaluated from the dependence of the grand potential on the chemical potential) is shown as a thick dotted line. The isotherm evaluated at $T^* = 1.2$ is continuous; this means that the critical temperature is lower than 1.2. More precise estimation leads to a critical temperature $T_c^* \simeq 1.19$ for a non-swelling system. The subsequent calculations have been carried out for a swelling system with $\alpha = 6$; this value of α is high enough to force relatively 'sharp' changes of the pore width for values of Γ close to G. Our calculations have been carried out for $T^* \geqslant 0.8$.

If the parameter $G = 0.5$ (i.e. the width of the pore equal to H_0 is attained for $\Gamma = 0.5$; for very much lower values of adsorption the pore is narrower—its width is somewhat higher than 4), no qualitative changes in the phase behaviour of the fluid within the temperature range investigated have been seen; cf. figure 4(a). In comparison with the adsorption isotherms shown in figure 3, the critical temperature is now slightly higher and equals $T_c^* \simeq 1.23$. This effect is connected with an increase of the pore width. Evidently, the isotherm evaluated at $T^* = 1.2$, which is displayed in figure 4(a), is subcritical, whereas the isotherm evaluated at the same temperature and plotted in figure 3 is supercritical. The changes of H accompanying the adsorption process are shown in figure 4(b). It is interesting that during capillary condensation the model leads to a continuous increase of the pore width along the adsorption branch, whereas during desorption the 'expanded' pore collapses abruptly at the end of the desorption branch of the hysteresis loop.

In figure 4(c) we show examples of density profiles. There are two profiles at the chemical potential $\mu/kT = -4.307\,09$; at this state point, two adsorbed phases coexist. Note that in

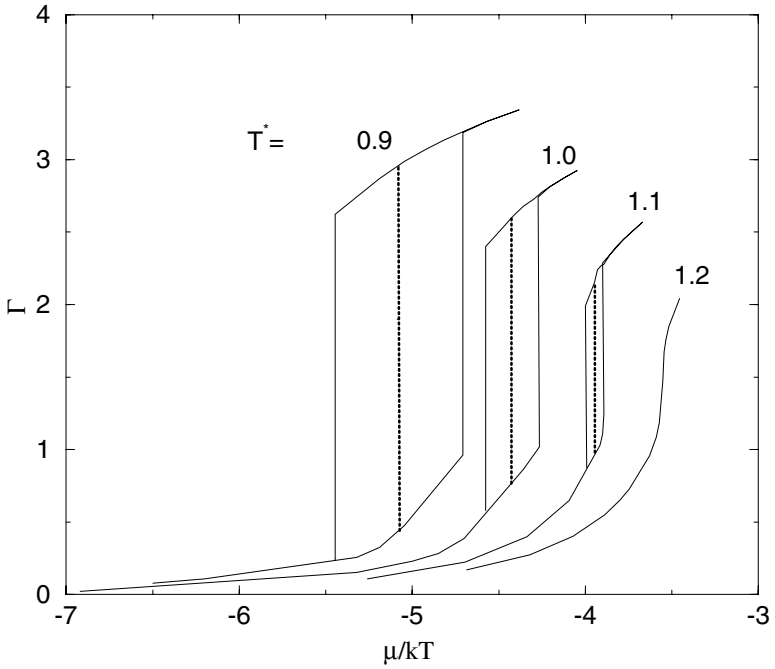

Figure 3. Adsorption isotherms at subcritical temperatures for rigid pores, $H_0 = 5$, $H_1 = 0$, $\varepsilon_s/\varepsilon = 10$ and $z_0 = 0.5$. The temperatures are listed in the figure.

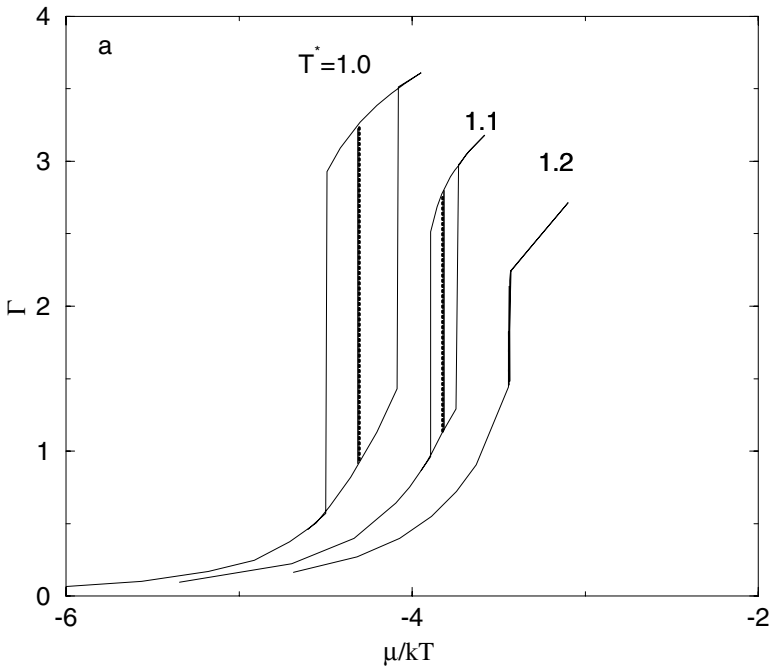

Figure 4. Adsorption isotherms (a), the dependence of H on μ (b) and the density profiles (c). The calculations are for $\alpha = 6$, $G = 0.5$. For all curves, $H_0 = 5$, $H_1 = 1$, $\varepsilon_s/\varepsilon = 10$ and $z_0 = 0.5$. The values of all remaining parameters are listed in the figures.

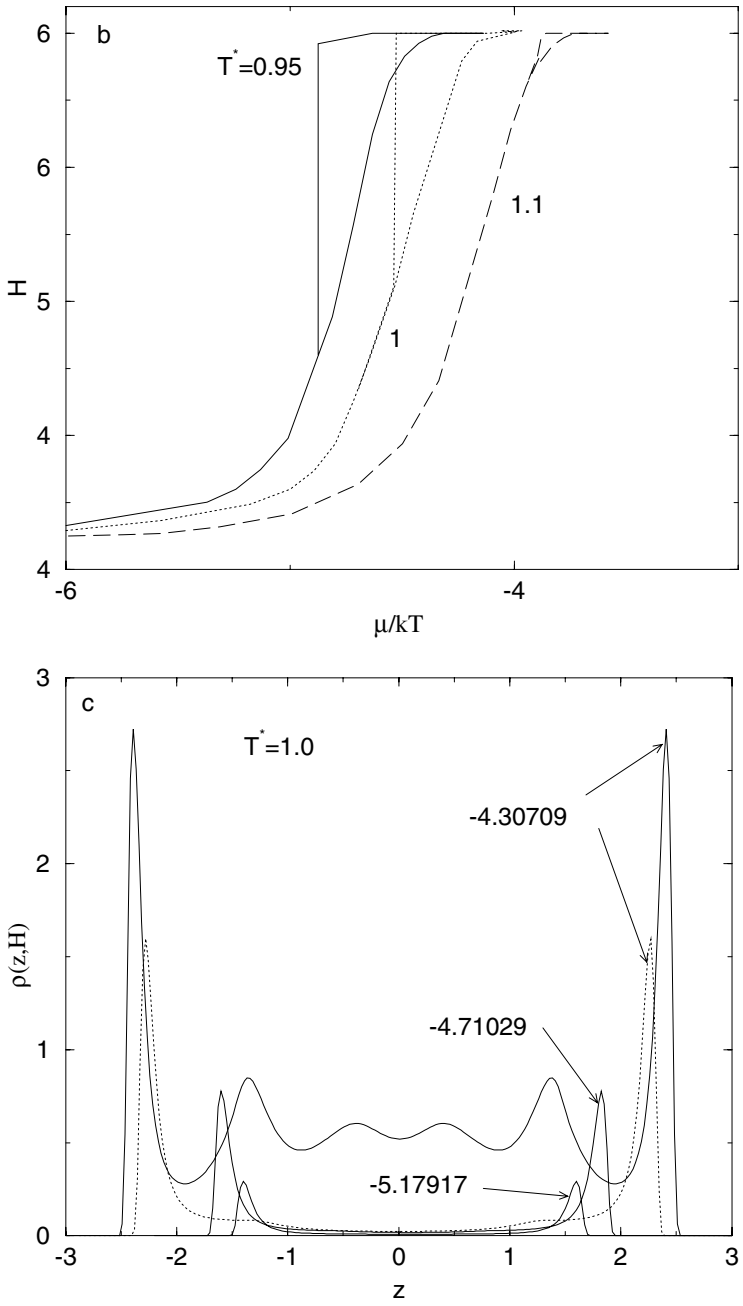

Figure 4. (Continued)

the case of an adsorbed liquid-like phase, the pore is somewhat wider than in the case of a gas-like adsorbed phase, i.e. the coexistence occurs between phases confined in pores of different widths.

The data presented in figure 5 were obtained for $G = 2.5$. Part (a) displays adsorption isotherms, part (b) gives an insight into the changes in the structure of adsorbed fluid, while

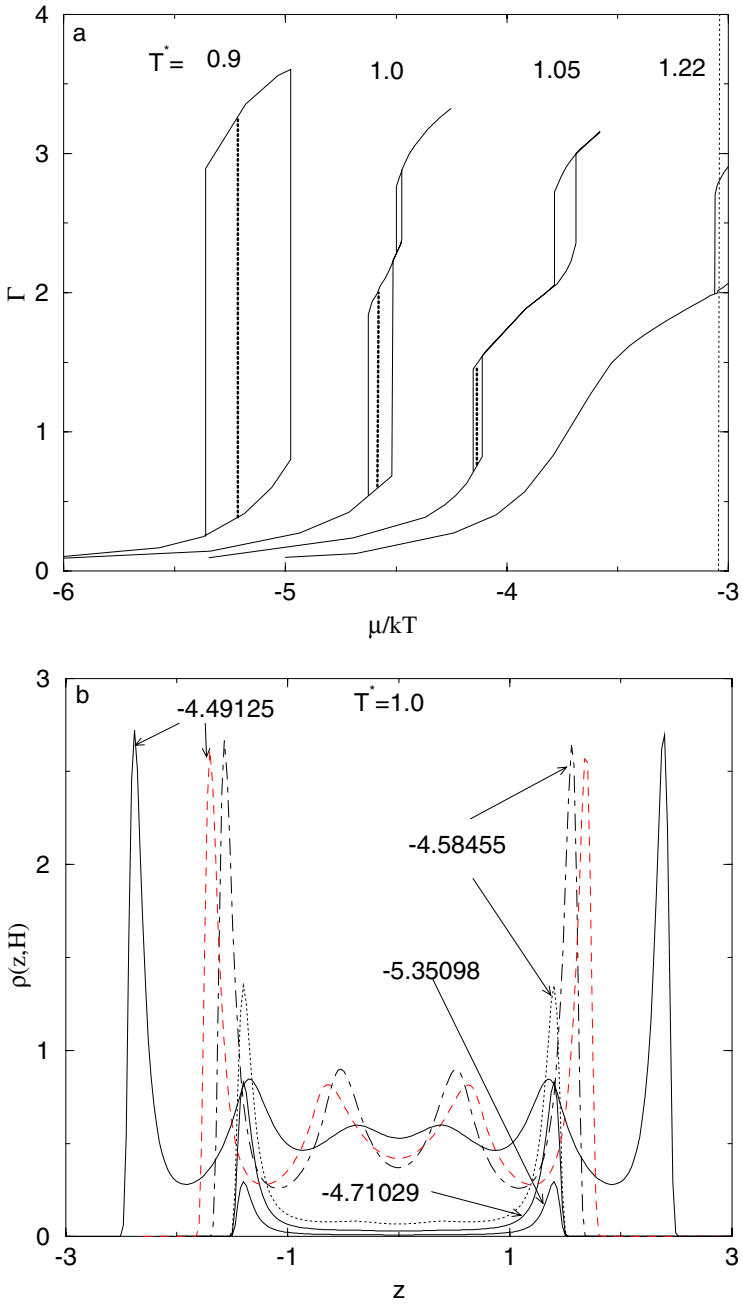

Figure 5. Adsorption isotherms (a), density profiles (b) and the dependence of Ω on μ (c). The calculations are for $\alpha = 6$, $G = 2.5$. For all curves, $H_0 = 5$, $H_1 = 1$, $\varepsilon_s/\varepsilon = 10$ and $z_0 = 0.5$. The values of all remaining parameters are listed in the figures.

part (c) shows an example of a plot of the grand potential (per unit of the surface area of one pore wall, A). From the adsorption isotherms for a rigid pore shown in figure 3, we learn that at higher temperatures the adsorption value $\Gamma = 2.5$ is attained at chemical potentials

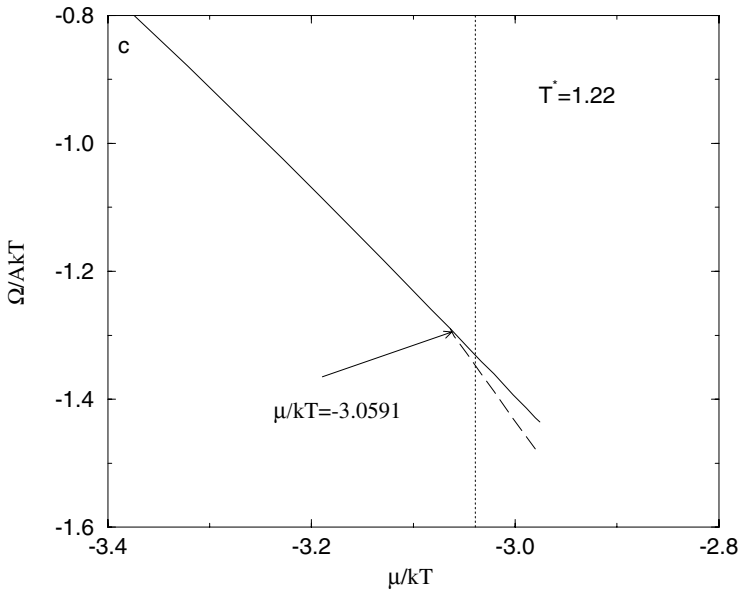

Figure 5. (Continued)

higher than the value of the chemical potential at the phase transition point. The adsorption isotherms plotted in figure 5(a) are qualitatively different from those shown in figures 3 and 4(a). Only at $T^* = 0.9$ is there a single adsorption loop; at higher temperatures two loops are seen. A scenario for phase changes in the system considered is illustrated in figure 5(b), where examples of the density profiles evaluated at $T^* = 1$ are given. Because of a rather high value of α, the pore is 'resistant' to the volume changes, unless the adsorption $\Gamma \simeq 2.5$ is attained. Thus, the first transition takes place in a pore somewhat wider than 4. Despite the pore volume showing resistance to expansion as long as the adsorption is lower than G, the phase condensation in that pore causes a slight increase of its width. In figure 5(b) there are shown two density profiles evaluated at the configurational chemical potential $\mu = -4.584\,55$; one of them (plotted as a dotted line) illustrates the structure of a rarefied phase, whereas the second profile (plotted as a dash–dotted line) is for the condensed phase. The formation of this phase is accompanied by a slight expansion of the pore. Further increase of the chemical potential leads to more rapid changes of the pore width, but the average density of the fluid inside the pore remains high. During pore expansion we do not observe any decompression of the adsorbed fluid; however, the maximum pore width change allowed by the model parameters is rather small—after the capillary condensation, the pore width changes from about 5 to 6. However, these width changes are different during adsorption and desorption and we observe the existence of an adsorption loop. The coexistence between phases adsorbed in pores of different widths occurs at $\mu/kT = -4.491\,25$.

For higher temperatures, the separation of the two adsorption loops becomes more pronounced as the chemical potential increases. At $T^* = 1.05$ the first hysteresis loop becomes narrower, but the second becomes wider. The first loop vanishes at $T^* \simeq 1.08$; i.e. this temperature is the critical temperature for that transition. The second loop still exists. At the temperature 1.225 the second adsorption loop approaches the value of the chemical potential at which bulk coexistence between gas and liquid phases has its onset (the locus of the bulk transition is marked by a vertical dotted line in figure 5(a)). The adsorption branch

of this loop is already located inside the bulk liquid–vapour coexistence region. In figure 5(c) we show the dependence of the grand potential Ω on the chemical potential μ at $T^* = 1.22$. Like in figure 5(a), a dotted vertical line shows the value of the chemical potential at the bulk liquid–vapour coexistence. The two branches—one for the expanded ('swollen') pore (dashed line) and the second for the narrower 'collapsed' pore (solid line)—meet at $\mu/kT = -3.0591$. However, these two branches do not form a 'typical' van der Waals loop. A similar situation occurs at other temperatures; i.e. the left-hand (desorption) branches of the second loops of the isotherms plotted in figure 5(a) determine the equilibrium between fluids adsorbed in 'swollen' and 'collapsed' pores. It is interesting to note that Ball and Evans [41], considering a different system, namely an adsorbent with a random distribution of pore sizes, found a continuous growth of the adsorption on increasing the chemical potential but a discontinuous jump in the desorption branch.

Figure 6 summarizes our results. We have plotted here the phase diagrams in the chemical potential–temperature plane for the systems investigated in figures 3–5. Additionally, we have also plotted the bulk coexistence curve. The solid lines with the labels '2' and '3' are for the systems that show a single transition (within the range of temperatures investigated). Curve 1 (for a swelling system, with $G = 2.5$) is composed of two branches, marked as solid and dotted lines. The latter corresponds to the 'expanding transition'. It starts at a triple-like point (the temperature of this point is approximately 0.945) and ends meeting the bulk coexistence line at $T^* = 1.224$. At higher temperatures it is still possible to calculate the isotherms exhibiting the 'expansion–collapse' loop, but this loop becomes metastable with respect to the bulk coexistence. Curve 3 is also for the 'expanding' pore, but now $G = 0.5$. Finally, curve 2 is for the pore with rigidly fixed positions of two walls; the width of this pore is $H = 5$.

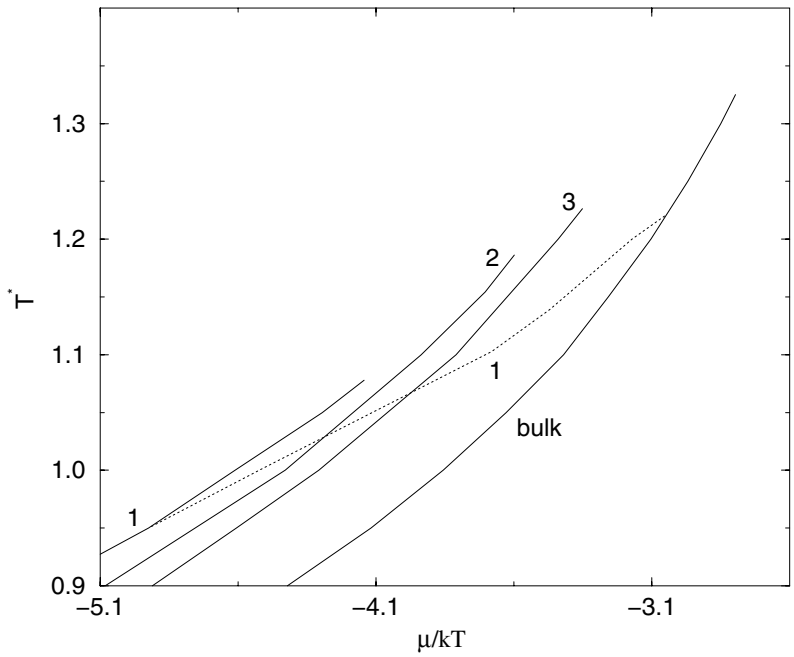

Figure 6. The phase diagram in the temperature–chemical potential plane. The branches are for the following systems: 1: $\alpha = 6$, $G = 2.5$; 2: non-swelling system, $H_1 = 0$; 3: $\alpha = 6$, $G = 0.5$. The values of the remaining parameters are given in the text. The curve marked 'bulk' denotes the bulk coexistence line.

The behaviour of system 1 is unusual. The critical temperature of the first transition (at a lower value of the chemical potential, $T_c^* \simeq 1.08$) is lower than the critical temperature of the second transition. Moreover, at low temperatures (e.g. at $T^* = 0.9$; cf. figure 5(a)) there exists only one transition in the system; thus the second transition is delimited by two temperatures: lower and upper.

The first transition is just the usual capillary condensation. At low temperatures the value of G lies 'inside' the capillary condensation loop and the condensation is accompanied by pore expansion. This situation persists up to the triple-like temperature, $T_t^* = 0.945$. When the temperature is raised above T_t^*, the adsorption Γ at the end of the capillary condensation loop becomes lower than G. In such a case the capillary condensation occurs in the 'collapsed' pore whose width changes a little during the transition. Consequently, the critical temperature for that transition is close to the critical temperature for a rigid, 'entirely collapsed' ($H = 4$) pore. Obviously, the critical temperature for a rigid pore whose width is the same as that of an 'entirely expanded pore' ($H = 6$) is higher than for the collapsed pore and equals $T_c^*(H = 6) = 1.235$. Moreover, the capillary condensation in the rigid pore of width 6 occurs at higher values of the chemical potential than that in the rigid pore of width 4. Thus, if the adsorption in system 1 increases above G at temperatures lower than the critical temperature ($T_c^* = 1.224$) but higher than T_t^*, the pore expands and the second transition develops. As we have already noted, in the case of this transition the desorption branch describes the chemical equilibrium in the system.

In this work we have proposed the application of the density functional approach to investigate adsorption in pores whose width can vary with the amount of adsorbed fluid. The dependence of the pore width H was assumed *ad hoc*; it has no theoretical justification. However, the proposed function reproduces qualitatively experimental observations. According to the calculations reported above, allowing for the possibility of pore width changes may lead to qualitative changes in the phase behaviour of the system.

Acknowledgment

This work was supported by KBN under grant No 3T09A08216.

References

[1] Evans R 1990 *J. Phys.: Condens. Matter* **2** 8989
[2] Gelb L D, Gubbins K E, Radhakrishnan R and Śliwińska-Bartkowiak M 1999 *Rep. Prog. Phys.* **62** 1573
[3] Dietrich S 1999 *New Approaches to Problems in Liquid State Theory* ed C Caccamo, J Hansen and G Stell (Amsterdam: Kluwer Academic) pp 199–244
[4] Schön M 2000 *Computational Methods in Surface and Colloid Science* ed M Borówko (New York: Dekker) pp 1–76
[5] Hyde S T 1995 *Colloids Surf.* A **103** 227
[6] Escobedo F A and de Pablo J J 1999 *Phys. Rep.* **318** 85
[7] Erman B and Mark J E 1997 *Structures and Properties of Rubberlike Networks* (New York: Oxford University Press)
[8] Mark J E and Erman B 1988 *Rubberlike Elasticity. A Molecular Primer* (New York: Wiley)
[9] Geissler E, Horkay F and Hecht A M 1994 *J. Chem. Phys.* **100** 8418
[10] Fontell K 1974 *Liquid Crystals and Plastic Crystals* ed G W Gray and P A Winsor (Chichester: Ellis Horwood)
[11] Escobedo F A and de Pablo J J 1996 *J. Chem. Phys.* **106** 793
[12] Escobedo F A and de Pablo J J 1997 *Mol. Phys.* **90** 437
[13] Grim R E 1960 *Applied Clay Mineralogy* (New York: McGraw-Hill)
[14] Tarasevich Ju I and Ovtscharenko F D 1975 *Adsorption on Clay Minerals* (Moskow: Naukova Dumka) (in Russian)
[15] Konta J 1995 *Appl. Clay Sci.* **10** 275

[16] Delville A and Sokołowski S 1993 *J. Phys. Chem.* **97** 6261
[17] Delville A 1993 *Langmuir* **8** 1796
[18] Delville A 1993 *J. Phys. Chem.* **97** 9703
[19] Delville A 1995 *J. Phys. Chem.* **99** 2033
[20] Skipper N T, Refson K and McConnell J D C 1991 *J. Chem. Phys.* **94** 7434
[21] Lee J Y, Baljon A R C and Loring R F 1999 *J. Chem. Phys.* **111** 9754
[22] Hackett E, Manias E and Giannelis E P 1998 *J. Chem. Phys.* **108** 7410
[23] Kawamura K, Ichikawa Y, Nakano M, Kitayama K and Kawamura H 1999 *Eng. Geol.* **54** 75
[24] Van Olphen H 1963 *Proc. 11th Natl Conf. on Clays and Clay Minerals* (Oxford: Pergamon) p 178
[25] Van Olphen H 1970 *Proc. Int. Symp. on Surface Area Determination (Bristol, 1969)* (London: Butterworth) p 255
[26] Frink L J D and van Swol F 1994 *J. Chem. Phys.* **100** 9106
[27] Frink L J D and van Swol F 1997 *J. Chem. Phys.* **106** 3782
[28] Kokkoli E and van Swol F 1998 *J. Chem. Phys.* **108** 4675
[29] Tvardovski A V, Fomkin A A, Tarasevich Yu I and Zhukova A I 1999 *J. Colloid Interface Sci.* **212** 426
[30] Laird D A, Shang C and Thompson M L 1994 *J. Colloid Interface Sci.* **171** 240
[31] Tarasevich Yu I, Telitschkun W P and Ovtscharenko F D 1972 *Kolloid Zh.* **34** 412
[32] Tarasevich Yu I 1971 *Ukr. Khem. Zh.* **37** 895
[33] Kamei G, Oda C, Mitsui S, Shibata M and Shinozaki T 1999 *Eng. Geol.* **54** 15
[34] Dekany I, Farkas A, Kiraly Z, Klumpp E and Narres H D 1999 *Colloids Surf.* A **119** 7
[35] Dekany I and Haraszti T 1997 *Colloids Surf.* A **123** 391
[36] Evans R 1992 *Fundamentals of Inhomogeneous Fluids* ed D Henderson (New York: Dekker) ch 3
[37] Zhou S 2000 *J. Chem. Phys.* **113** 8717
[38] Tarazona P 1985 *Phys. Rev.* A **31** 2672
Tarazona P 1985 *Phys. Rev.* A **32** 3148 (erratum)
[39] Weeks D, Chandler D and Andersen H C 1977 *J. Chem. Phys.* **54** 5237
[40] Lee L L 1988 *Molecular Thermodynamics of Non-ideal Fluids* (London: Butterworth)
[41] Ball P C and Evans R 1989 *Langmuir* **5** 714